ESJ Natural/Life/Medical Sciences Peer-reviewed

Dynamics of Water Erosion in the Aghien Lagoon Catchment

Ehouman Serge Koffi
Amidou Dao
Dabissi Djibril Noufe
Mamadi Ouedraogo
Nagnon Bernard Yeo
Laboratoire de Géosciences et Environnement,
Université Nangui Abrogoua, Côte d'Ivoire
Luc Seguis
Jean Louis Perrin
IRD, UMR Hydrosciences, Université de Montpellier 2, France
Bamory Kamagate
Lancine Droh Gone
Laboratoire de Géosciences et Environnement,
Université Nangui Abrogoua, Côte d'Ivoire

Doi:10.19044/esj.2024.v20n33p187

Submitted: 20 June 2024
Accepted: 20 November 2024
Published: 30 November 2024

Copyright 2024 Author(s)
Under Creative Commons CC-BY 4.0
OPEN ACCESS

Cite As:
Koffi E.S., Dao A., Noufe D.D., Ouedraogo M., Yeo N.B., Seguis L., Perrin J.L., Kamagate B. & Gone L.D. (2024). *Dynamics of Water Erosion in the Aghien Lagoon Catchment*. European Scientific Journal, ESJ, 20 (33), 187.
https://doi.org/10.19044/esj.2024.v20n33p187

Abstract

Soil erosion significantly impacts land quality and water resources. This paper focuses on estimating spatiotemporal changes in land-use/land-cover patterns and soil erosion in the Aghien lagoon watershed in Côte d'Ivoire. The study utilized Landsat imagery from 2016 and 2020. Images were classified into categories using supervised classification with the maximum likelihood algorithm. The Universal Soil Loss Equation (USLE) model was applied in a GIS environment to quantify potential soil erosion risk. The areas of bare soil/habitats and crops/fallow increased by 2,981 ha (37.8%) and 2,642 ha (17.58%), respectively, between 2016 and 2020. High soil losses were observed on the slopes of rivers and valleys adjacent to the Aghien lagoon, which are naturally predisposed to erosion due to the steepness, length,

 ISSN: 1857-7881 (Print) e - ISSN 1857-7431

and inclination of the slopes. Average soil loss values were 60.65 t/ha/year in 2016 and 47.64 t/ha/year in 2020. Areas with very low and low soil loss values covered 34,441.52 ha (94.36%) in 2016 and 34,956.76 ha (95.77%) in 2020. Conversely, areas with high and very high soil losses were minimal, accounting for 0.95% and 0.60% of the watershed in 2016 and 2020, respectively. Moderate soil erosion contributed most to soil loss, affecting 1,712.19 ha (4.69%) in 2016 and 1,305.77 ha (3.58%) in 2020.

Keywords: Erosion, lagoon Aghien, Abidjan, GIS

Introduction

Water erosion is a natural phenomenon and one of the primary factors contributing to soil degradation (Bouguerra et al., 2017). The intensification of soil degradation is influenced by several natural and anthropogenic factors that trigger and develop erosion processes. These factors are broadly categorized into two groups: quasi-static factors such as infiltration, erodibility, and morphology, and dynamic factors, including vegetation cover, land use, rainfall intensity, and agricultural practices (Roose & Lelong, 1976; Vrieling, 2005; Boukheir et al., 2006; Toumi et al., 2013).

In addition, climate change, population pressure (Mazouzi et al., 2021), and the expansion of cash crops have increased land exposure to runoff processes, consequently exacerbating soil degradation through erosion (Das et al., 2020). Various human activities, including agricultural practices, forestry, grazing, road construction (Belaout et al., 2021), and urban development, tend to modify and often accelerate erosion phenomena significantly (Wachal et al., 2009). Erosion results from the detachment and transport of soil or rock particles under the kinetic energy of raindrops (Kinnell, 2016; Benchettouh et al., 2021). This process degrades soil fertility, reduces water quality, diminishes reservoir capacity, and causes siltation of hydro-agricultural infrastructures (Kouassi et al., 2020; Khemiri & Jebari 2021). The impacts of soil erosion are far-reaching, including reduced soil productivity, degraded water quality due to eutrophication, siltation, and sedimentation of lakes and river beds, increased flood risks, and more (Onyando et al., 2005; Zhou et al., 2008; Das et al., 2020).

In Côte d'Ivoire, early studies on land erosion were conducted by Rougerie (1958, 1960) in forest regions, analyzing various erosion processes, factors, and anti-erosion methods. Subsequent studies on water erosion include investigations along the coast (Adopo et al., 2014; Abé et al., 2014) and in the Boubo coastal watershed (Coulibaly et al., 2021). Other studies focused on specific regions such as Bonoua (Aké et al., 2012), Adiaké (Eblin et al., 2017), Korhogo (Koukougnon et al., 2021), and Man (Kouadio et al., 2007). Research on watersheds includes the Lake Buyo watershed (Koua et

 ISSN: 1857-7881 (Print) e - ISSN 1857-7431

al., 2019), the Mé River (Kouadio et al., 2018), the Lobo River (Déguy et al., 2018), and the hydro-agricultural dam watershed of Babadou (Kouassi et al., 2020). N'Dri et al. (2017) conducted experiments in the Attécoubé commune within the autonomous district of Abidjan, demonstrating significant modifications to natural environments caused by erosion.

The population increase in the Autonomous District of Abidjan in recent years, driven by socio-political crisis and migration from rural areas and neighboring countries (Nana, 2018), has led to a high demand for housing. This demand has triggered widespread real estate development, often preceded by extensive earthworks that degrade vegetation cover. Once stripped of vegetation, the soil becomes vulnerable to climatic impacts.

This study applies the Universal Soil Loss Equation (USLE) model in conjunction with a Geographic Information System (GIS), an approach that facilitates the estimation of water erosion and its spatial distribution over large areas, including watersheds, countries, or even continents (Khemiri & Jebari, 2021).

The objective of this manuscript is to analyze and spatialize the factors contributing to erosion, creating a thematic map of erosion risks and soil losses in the Aghien lagoon catchment area. Identifying vulnerable areas through the soil loss map will enable decision makers to implement protective measures and ensure efficient management of the Aghien lagoon.

Material and Methods

Study Area

The Aghien lagoon watershed is located in the North-East of Côte d'Ivoire (Diallo et al., 2018), on the outskirts of the autonomous district of Abidjan, between longitudes 375,000 m and 410,000 m West and latitudes 598,000 m and 619,000 m North. It is a peri-urban basin that straddles three (03) communes of the district. The area is urbanized, encompassing the most populated neighborhoods of the commune of Abobo, and has a total surface area of 365 km². It comprises two basins drained by the Djibi and Bété rivers, tributaries of the Aghien lagoon. The Bété basin covers an area of 216 km², while the Djibi basin spans 78 km² (Diallo et al., 2018).

The regional climate is influenced by the seasonal movement of air masses over the south-eastern region. Very dry tropical continental air, known as the Harmattan, flows southward from the Sahara, while humid maritime equatorial air, called the monsoon, originates from the St Helena high-pressure system. The interplay between these two air masses governs the climate of the study area, dividing it into four major seasons that define the hydrological cycle. These include two rainy seasons (May–July and October–November), and two dry periods (July–September and December–April) (Koffi et al., 2019).

 ISSN: 1857-7881 (Print) e - ISSN 1857-7431

The sedimentary basin encompassing much of the Aghien lagoon's catchment area forms a large, flattened crescent along the Atlantic coast, stretching from Sassandra to Ghana. It extends about 45 km inland, with an elevation not exceeding 130 m, and spans a surface area of approximately 8,000 km². The sedimentary basin dates back to the Cretaceous-Cenozoic, Meso-Cenozoic, and Paleoproterozoic eras and primarily consists of clayey sands and coastal sands. It is traversed by the lagoon fault, a major geological feature with a displacement of nearly 3,000 m (Kouassi, 2013; Traoré, 2016).

The eastern edge of the Aghien lagoon is characterized by Quaternary sands and muds. Sands, clays, and ferruginous sandstones from the Continental Terminal (Tertiary) period are the most prevalent.

The slopes within the Aghien catchment area range from 0 and 20°, with an average slope of 4° and a standard deviation of 2.8°. Generally, the slopes are low. The gentlest slopes are located in the alluvial zones of the main tributaries, upstream of the catchment area, and in the urban areas on the plateaus near the Djibi. Steeper slopes are located along the edges of plateau incisions, descending sharply toward the lagoon (Koffi et al., 2019).

The vegetation in the study area is predominantly characterized by evergreen forest. This woody formation includes large trees, some of which are commercially available. However, the forest has undergone significant regression due to human activities, leading to its replacement by a mosaic of classified forests.

The vegetation along the borders of the Aghien lagoon primarily consists of swamp forest dominated by mangroves and bamboos. These vegetation types play a crucial role in stabilizing the lagoon environment by acting as a buffer zone, preventing the discharge of nutrients and sediments into the lagoon, and providing wildlife habitat (N'Dri et al., 2017).

The average monthly temperature in the region ranges between 24.7°C and 27.8°C. Higher temperatures are typically observed from February to April during the long dry season. The onset of the primary rainy season brings increased cloud cover, which leads to a temperature drop, with the lowest temperatures recorded in August (24.77°C).

 ISSN: 1857-7881 (Print) e - ISSN 1857-7431

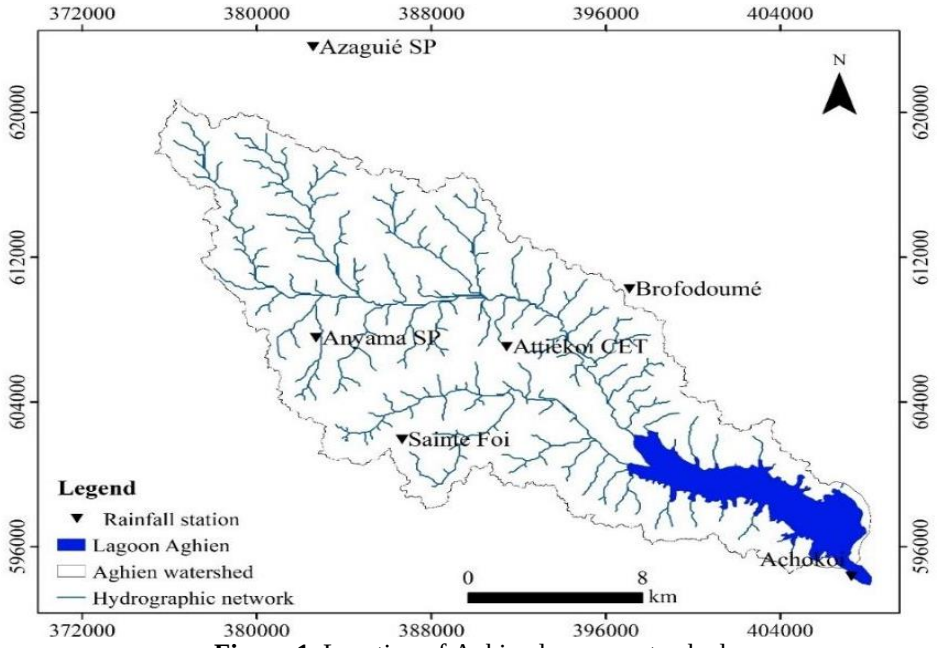

Figure 1. Location of Aghien lagoon watershed

Data Used

The annual rainfall for 2016 and 2020 was calculated using data collected from rainfall stations installed within the Aghien lagoon catchment area since 2015.

The years 2016 and 2020 were specifically chosen based on the availability of satellite imagery.

The distribution of R values was assumed to vary consistently with annual precipitation across the watershed. The highest annual R factor values were observed in areas with greater precipitation.

Figure 2 shows the annual rainfall values recorded at the various stations. In 2016, rainfall exceeded 2400 mm at most stations, including Anyama, Attiékoi CET, Achokoi, Brofodoumé, and Sainte Foi. The exception was the Azaguié station, where rainfall was recorded at approximately 1900 mm. Conversely, in 2020, the rainfall values were slightly above 2000 mm at the Achokoi station in the commune of Bingerville, as well as the Anyama and Sainte Foi stations in the commune of Abobo. Rainfall levels at the Azaguié, Brofodoumé, and Attiékoi CET stations, located on the periphery of the autonomous district of Abidjan remained below 2000 mm. Overall, rainfall levels in 2016 were generally higher than those observed in 2020.

 ISSN: 1857-7881 (Print) e - ISSN 1857-7431

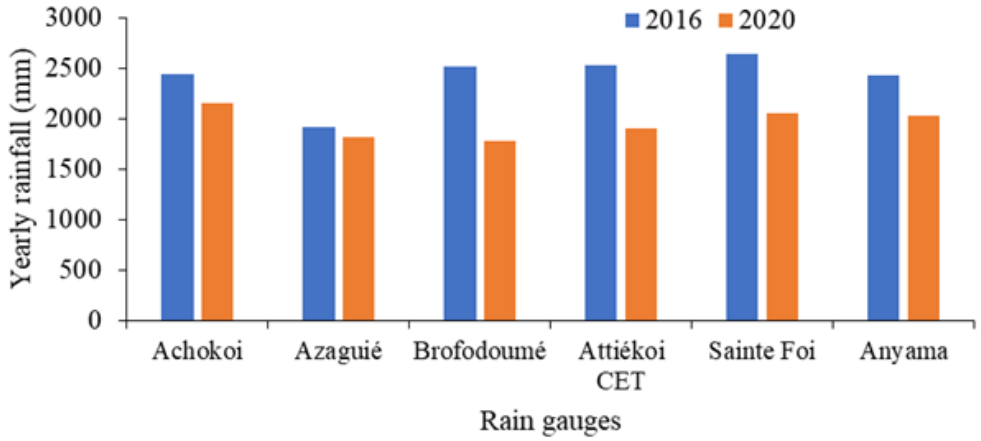

Figure 2. Annual rainfall at rain gauge stations in the Aghien lagoon catchment area

Satellite images from Landsat 8 (OLI) for the years 2016 and 2020 were downloaded from NASA's Earth Explorer website (**https://earthexplorer.usgs.gov**). The images were acquired at a 30-meter spatial resolution using the WGS 84 coordinate system. Landsat 8 band designations for the Operational Land Imager (OLI) are presented in Table 1, which also records the resolution of the images.

Table 1. The spatial resolution of Landsat 8 (OLI) images

Band Number	Description	Wavelength (µm)	Resolution
Band 1	Coastal / Aerosol	0.433 to 0.453	30
Band 2	Visible blue	0.450 to 0.515	30
Band 3	Visible green	0.525 to 0.600	30
Band 4	Visible red	0.630 to 0.680	30
Band 5	Near-infrared	0.845 to 0.885	30
Band 6	Short wavelength infrared	1.56 to 1.66	30
Band 7	Short wavelength infrared	2.10 to 2.30	30
Band 8	Panchromatic	0.50 to 0.68	30
Band 9	Cirrus	1.36 to 1.39	30
Band 10	Long wavelength infrared	10.3 to 11.3	100
Band 11	Long wavelength infrared	11.5 to 12.5	100

Table 2. Satellite images used

Acquisition data	Sensor	Path/row
05/01/2016		
28/01/2016	Landsat 8 OLI/TIRS	196-56 and 55
07/01/2020		

 ISSN: 1857-7881 (Print) e - ISSN 1857-7431

Land Use Change Rate

The vegetation classes or land cover were mapped using supervised classification of a Landsat 8 OLI multispectral image. Pre-processing steps included correction, combination, and masking. After creating ROI areas, a supervised maximum likelihood classification was performed, assigning pixels to classes based on reflectance probabilities. A confusion matrix validation produced a vegetation cover map with five classes.

The rate of land cover change between two dates was calculated using Diallo et al.'s (2018) formula:

$$T = \frac{V_f - V_i}{V_f}$$

Where T: Rate of change of vegetation cover between two dates;
Vi: The proportion of the land cover class taken at the initial state;
Vf: The proportion of the land cover class taken at the final state.

Generation of the Thematic Maps of RUSLE Model

The Universal Soil Loss Equation (USLE) developed by Wischmeier and Smith (1978), estimates soil erosion in croplands or gently sloping areas (Ganasri & Ramesh, 2016). It integrates five factors: rainfall erosivity (R), soil erodibility (K), slope length (L), slope steepness (S), cover management (C) and conservation practices (P) (Renard & Freimund, 1994; Panagos et al., 2015a, 2015b; Benchettouh et al., 2021; Piyathilake et al., 2020; Khemiri & Jebari, 2021; Payet et al., 2012).
The equation is:

$$A = R * K * C * LS * P$$

Where: A: average annual soil loss (t/ha/year)
R: rainfall aggressiveness (MJ.mm/ha/hr/year)
K: soil erodibility factor (t/ha/MJ/mm/ ha.h)
LS: topographical factor (L = slope length, S= slope steepness)
C: vegetation and management factor (dimensionless)
P: conservation practice factor (dimensionless).

This empirical model is based on over 10,000 plot-years of sheet and rill erosion data (Roose, 1977).

 ISSN: 1857-7881 (Print) e - ISSN 1857-7431

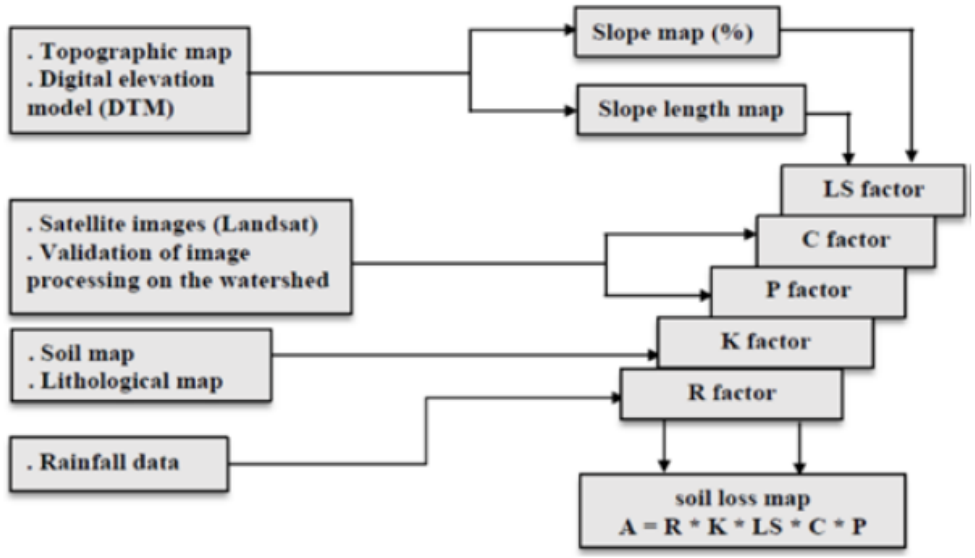

Figure 3. Methodology for estimating soil loss (Meliho et al., 2016)

Support Practice Factor (P)

The P factor is the ratio of soil loss from land with a specific support practice to that from an experimental plot with upslope and downslope tillage (Swarnkar et al., 2018). Anti-erosion practices include contour cultivation, strip or terrace farming, bench reforestation, and ridging (Table 3). P values range from 0 to 1, where 0 indicates strong resistance to human-induced erosion, and 1 reflects the absence of anti-erosion measures (El Garouani et al., 2008). The methodology is illustrated in Figure 4.

Table 3. Correspondence between slopes and the different types of crops recommended by Shin (1999)

Slope (%)	Crops in contour	Crops in band	Terrace with contour crops
0.0 – 7.0	0.55	0.27	0.10
7.0 – 11.3	0.60	0.30	0.12
11.3 – 17.6	0.80	0.40	0.16
17.6 – 26.8	0.90	0.45	0.18
26.8 >	1.00	0.50	0.20

Figure 4. Steps for mapping the P factor under Shin (1999)

 ISSN: 1857-7881 (Print) e - ISSN 1857-7431

Rainfall-runoff Erosivity Factor (R)

The R factor depends on rainfall–runoff characteristics, which are, in turn, influenced by geographic location. Therefore, the rainfall characteristics of the entire watershed (36,500 ha) were considered adequately represented by data collected from six weather stations within the study area. Rainfall data were gathered from these six meteorological stations in the study watershed between 2016 and 2020. Rainfall–runoff erosivity was determined using the method of Roose (1977, 1985), where P represents annual rainfall.

$$R = P * 0.6$$

The altitude map, derived from the 30 m DTM (**Figure 5**), shows that altitudes in the Aghien catchment area range from 0 m to 137 m. The highest altitudes are found in the commune of Abobo and the northern periphery of the catchment area, which together form the water divide. The lower altitudes are located toward the southern part of the catchment area, where they are more or less homogeneous and situated to the south-east of the Aghien lagoon watershed.

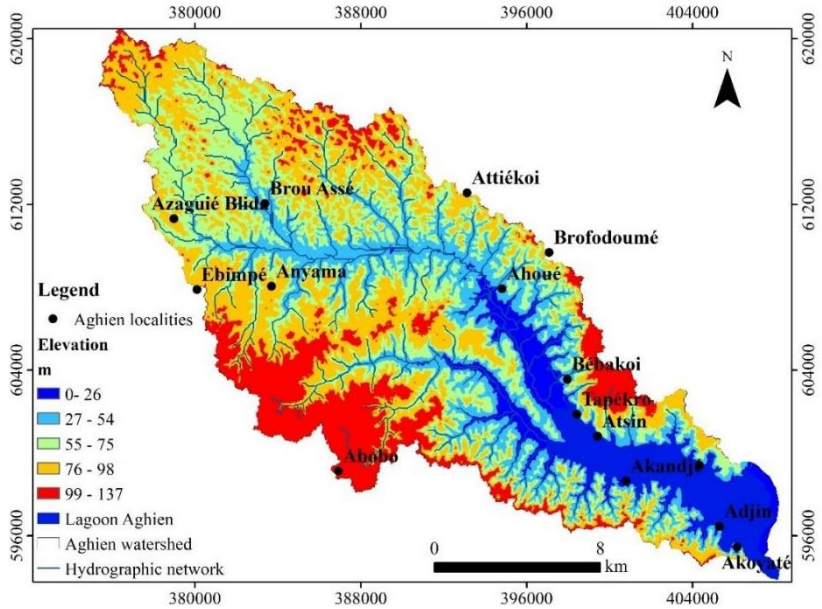

Figure 5. Elevation class map of Aghien lagoon watershed

Soil Erodibility Factor (K)

Erodibility refers to the rate of erosion caused solely by the inherent properties of the soil itself. The K-factor expresses the soil's susceptibility to erosion due to rainfall (Anache et al., 2015; Songu et al., 2021). The K-factor measures the vulnerability of soil particles to detachment and transport by rainfall and runoff. Texture is the primary factor influencing the K-factor, but soil structure, organic matter content, and permeability also play important roles (Stone & Hilborn, 2000; El Garouani et al., 2008; Markhi, 2015).

 ISSN: 1857-7881 (Print) e - ISSN 1857-7431

Table 4. General sensitivity of soil texture to erosion (Stone & Hilborn, 2000)

Area soil class	Relative sensitivity to water erosion	OM content			Correspondence of the soils in the Aghien watershed
		< 2 %	> 2 %	Average	
Very fine sand	Very high	0.46	0.37	0.43	
Very fine loamy sand	High	0.44	0.25	0.39	
Silty loam		0.41	0.37	0.38	
Very fine sandy loam		0.41	0.33	0.35	
Silt-clay loam		0.35	0.30	0.32	
Clay Loam		0.33	0.28	0.30	
Loam		0.34	0.26	0.30	
Silty clay	Moderate	0.27	0.26	**0.26**	Ferrallitic sandy-clay soil
Clay		0.24	0.21	**0.22**	Hydromorphic soil
Sandy clay loam		–	0.20	0.20	
Heavy clay		0.19	0.15	0.17	
Loamy sand	Slight	0.05	0.04	**0.04**	Ferrallitic sandy-clay soil
Fine loamy sand		0.15	0.09	**0.11**	Complex ferrallitic soil
Fine sand		0.09	0.06	0.08	
Coarse sandy loam		–	0.07	**0.07**	Sandy ferrallitic soil
Sandy loam	Very light	0.14	0.12	0.13	
Sand		0.03	0.01	0.02	

Cover-management Factor (C)

Soil that is well protected by vegetation cover significantly reduces the effects of climatic aggressiveness, soil erodibility, and slope gradient, regardless of their importance. Appropriate cover facilitates infiltration, thus reducing runoff and preventing erosion (Meliho et al., 2020).

The C-factor reflects the effect of cropping and management practices on soil erosion rates in agricultural lands and the effects of vegetation canopy and ground cover on reducing soil erosion in forested regions (Renard et al., 1996; Meliho et al., 2020). In recent years, due to the large spatial and temporal variability of vegetation cover, satellite images have been used to extract the C-factor (Karydas et al., 2009; Tian et al., 2009).

The C-factor expresses the weighted ratio of soil losses over a land use situation to those measured in a unit plot (Renard et al., 1996; Batista et al., 2017). Therefore, it reflects not only land use, but also crop type, tillage practices, and other conservation conditions (Panagos et al., 2015a). Values of the C-factor range from 0 to 1.0, with lower values corresponding to densely vegetated landscapes, such as forested areas, and higher values corresponding to bare soil.

 ISSN: 1857-7881 (Print) e - ISSN 1857-7431

For catchment-scale erosion modelling, C-factor values can be assigned to land use classes (Panagos et al., 2015a, 2015b). In this study, land cover maps were produced using Landsat 8 Surface Reflectance images with a 30 m resolution, dated 2016 and 2020. A supervised classification was performed to obtain the cover classes (Trimble, 2010). Finally, C-factor values were assigned to the identified land use classes (Table 6).

Table 5. Land use coefficient C as a function of land use type [38] (Payet et al., 2012)

Type of land use	C-Factor
Bare soil	1
Degraded forest	0.7
Savannah with trees and shrubs	0.3
Degraded Grass Savannah	0.6
Mosaic of culture	0.5
Mangrove	0.28
Habitats	0.2
Wooded area	0.18
Paddy field	0.15
Dense forest	0.001
Water bodies	0

Topographic Factor (LS)

Topography is one of the main factors in soil erosion and hydrological modeling because it defines the effect of gravity on the movement and flow of water and sediments. The length (L) and steepness of the slope (S) affect sediment yield (Meliho et al., 2020).

The topographic factor (LS) depends on both the slope length (L) and slope steepness (S). Erosion increases with the length and inclination of the slopes (Bollinne & Rosseau, 1978; Bollinne & Laurant, 1983). The calculation of the LS-factor for the Aghien lagoon is carried out on a GIS platform. The latter uses the DEM (Digital Elevation Model) to calculate the slope in degrees, orientation, and cumulative length. The combination of the L and S factors gives the LS factor. The LS-factor is a ratio of soil loss under given conditions to soil loss at a location with a "standard" slope of 9% and a slope length of 22.1 m. The steeper and longer the slope, the higher the erosion risk (Wischmeier & Smith, 1978). The formula used was developed by Desmet and Govers (1996). Topography plays a significant role in erosion and landslide. The topographic factor (LS) depicts the effects of topography on erosion, including the length and steepness of the slope that influence the surface runoff speed (Biswas & Pani, 2015).

$$L = ((A + D^2)^{m+1} - A^{(m+1)})/(X^m D^{(m+2)} * 22.1^m \quad (1)$$

Where A (m) is the area at the input of a pixel (cell), D is the pixel size, and x is the shape correction factor.

 ISSN: 1857-7881 (Print) e - ISSN 1857-7431

$$m = \frac{F}{F+1} \tag{2}$$

$$F = (\frac{\frac{sin\ sin\ ("slope" * 0.01745)}{0.0896}}{3 * power(sin\ sin\ ("slope" * 0.01745)\ ,0.8) + 0.56} \tag{3}$$

$$S = 10.8 * sin\theta + 0.03\ for\ slope < 9\% \tag{4}$$

$$S = 16.8 * sin\theta - 0.05\ for\ slope \tag{5}$$

The slopes of the Aghien catchment area range from 0° to 35.5°, with an average of 6.2° and a standard deviation of 4.7°. The slopes are generally low. The very low and low slopes occupy 95.95% of the surface area of the Aghien catchment area and are located in the alluvial zones of the main tributaries, in the upstream part of the catchment area, and in the urban areas on the plateaus of the Djibi River. On the other hand, steep slopes are found at the edges of the plateau incisions facing the lagoon (**Koffi et al., 2014**) and are also found on the slopes of the Bété and Djibi rivers. Steep and very steep slopes occupy 0.22% of the study area (**Table 6 and Figure 6**).

Figure 6. Slope map of Aghien lagoon watershed

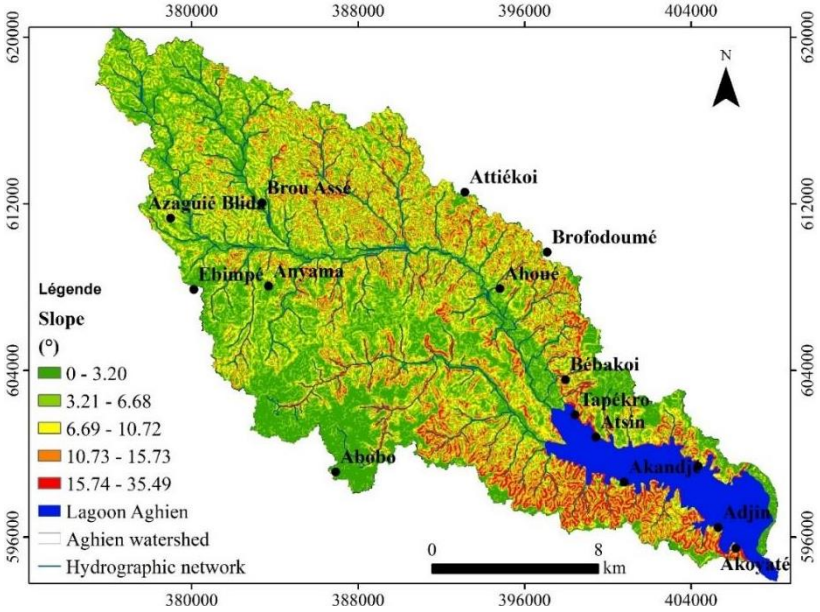

 ISSN: 1857-7881 (Print) e - ISSN 1857-7431

Table 6. Declivity classes

Slope (°)	Area (ha)	Area (%)	
0-3.20	25922.32	71.02	Very low
3.21-6.68	9097.63	24.93	Low
6.69-10.72	1400.49	3.84	Moderate
10.73-15.73	76.31	0.21	High
15.74-35.49	3.25	0.01	Very high

All the factors in the USLE equation proposed by Wischmeier and Smith (1978) were interpolated using ArcGis software.

Results and Discussion

Land Use

The land use map (**Figures 7**A and 7B) was prepared based on the land use cover map of the study area. The land use was classified into five main classes: water body, forest area, degraded forest, crops/fallow, and bare soil. In 2016, the Aghien lagoon watershed was dominated by degraded forest and crops/fallow land (**Figure 7**A), with respective areas of 16,011 ha and 12,384 ha, accounting for 44.81% and 33.92% of the total watershed area. By 2017, the area of degraded forest had decreased to 11,122 ha (30.4%), representing a reduction of 4,889 ha. This loss was primarily replaced by an increase in crops/fallow land, which expanded to 15,026 ha (41.15%), an increase of 2,642 ha. This regression in degraded forest also contributed to an increase in habitat area, which grew from 4,906 ha in 2016 to 7,887 ha in 2017 across the entire watershed (**Table 8**). Bare soil and habitats were concentrated in the southern part of the watershed, predominantly in the communes of Anyama and Abobo. The few forested areas in the study region were small pockets of classified forest, which are being gradually destroyed in favour of industrial crops and the expansion of the autonomous district of Abidjan. Forested areas decreased from 1,253 ha (3.43%) in 2016 to 540 ha (1.48%) in 2017, a decline of 713 ha. Meanwhile, the surface area of the lagoon water body experienced minimal variation, shrinking slightly from 1,957 ha in 2016 to 1,936 ha in 2017.

 ISSN: 1857-7881 (Print) e - ISSN 1857-7431

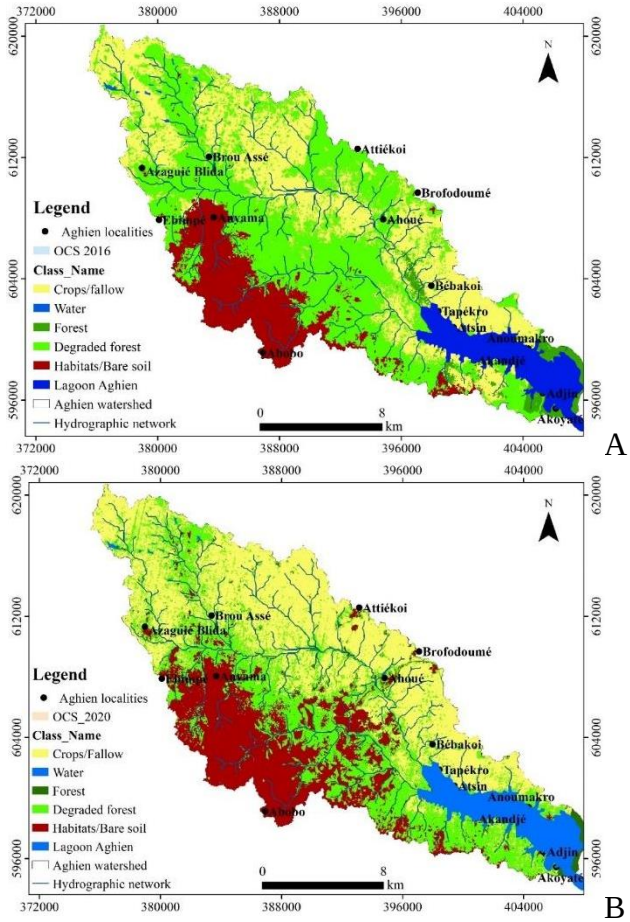

Figure 7. Land use/land cover in Aghien lagoon watershed (A: 2016; B: 2020)

Table 7. Land use class

	2016		2020		2016-2020	
Class name	Area (ha)	Area (%)	Area (ha)	Area (%)	Area change (ha)	Area (%)
Soil Bare/Habitat	4906	13.44	7887	21.60	2981	37.80
Forest	1253	3.43	540	1.48	-713	-132.04
Water	1957	5.36	1936	5.3	-21	-1.08
Crops/Fallow	12384	33.92	15026	41.15	2642	17.58
Forest Degraded	16011	43.85	11122	30.46	-4889	-43.96

USLE Factor Mapping

Rainfall Erosivity Factor (R)

The average annual rainfall erosivity factor (R) for the six weather stations ranged from 1,145 to 1,583 MJ mm ha^{-1} hr^{-1} $year^{-1}$ in 2016 and from 1,068 to 1,290 MJ mm ha^{-1} hr^{-1} $year^{-1}$ in 2020 (**Table 4; Figures 8**A and 8B).

 ISSN: 1857-7881 (Print) e - ISSN 1857-7431

The average R-factor values were 1,478 MJ mm ha^{-1} h^{-1} $year^{-1}$ in 2016 and 1,175 MJ mm ha^{-1} h^{-1} $year^{-1}$ in 2020 (**Table 8**).

Thematic maps of the R-factor were classified into five categories: very low, low, moderate, high, and very high. This classification was applied to all thematic maps of the USLE model.

Table 8. *Rainfall erosivity (R) values*

	2016 Rainfall (mm)	R (MJ mm ha^{-1} hr^{-1} $year^{-1}$)	2020 Rainfall (mm)	R (MJ mm ha^{-1} hr^{-1} $year^{-1}$)
Achokoi	2437.30	1462.38	2150.5	1290.3
Azaguié	1909.00	1145.40	1818.2	1090.92
Brofodoumé	2509.80	1505.88	1780	1068
Attiékoi CET	2527.30	1516.38	1907	1144.2
Sainte Foi	2638.50	1583.10	2050	1230
Anyama	2425.70	1455.42	2024.3	1214.58

The spatial distribution for 2016 shows that the lowest erosivity values are confined to the northern part of the catchment area, specifically in the Brou Assé region. In contrast, the highest values are concentrated in the central part of the catchment, while areas with high erosivity are located on either side of these peaks. Moderate erosivity values are bordered by both low and high erosivity zones (**Figure 8**).

For 2020, the spatial distribution reveals a map largely devoid of high and very high erosivity zones (**Table 9; Figure 8**B). The northern part of the catchment, encompassing villages such as Ahoué and Attiékoi, is predominantly covered by very low erosivity. In the southern region, including communes like Abobo and Anyama, low erosivity is observed. Moderate erosivity is confined to the eastern section of the Aghien lagoon watershed.

This spatial distribution underscores the heterogeneous nature of erosivity, which may also reflect the variability in rainfall recorded at the different rainfall stations.

 ISSN: 1857-7881 (Print) e - ISSN 1857-7431

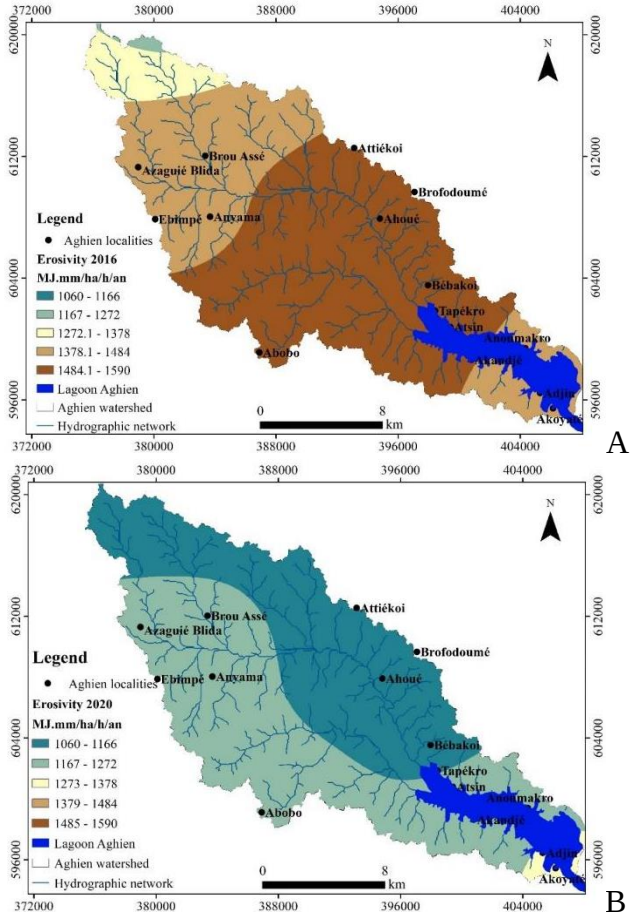

Figure 8. Spatial distribution of the R factor in Aghien lagoon watershed (A: 2016; B: 2020)

Table 9. R-factor distribution in Aghien lagoon watershed

	2016			2020		
R factor (MJ.mm/ha/hr/year)	**Area (ha)**	**Area (%)**	**Average (MJ.mm/ha/hr/year)**	**Area (ha)**	**Area (%)**	**Average (MJ.mm/ha/hr/year)**
1066 – 1166	0.09	0.00		15746.13	43.14	
1167 – 1272	196.72	0.54		19886.37	54.48	
1273 – 1378	2459.70	6.74	1478.1	867.50	2.38	1175.6
1379 – 1484	13280.02	36.38				
1485 – 1590	20563.47	56.34				

Topographic Factor (LS)

The values of the LS factor range from 0 to 15. The very low and low classes (0 - 3.18) dominate the catchment, covering 81.65 % of the area. Moderate LS values (3.19-5.68) account for 15.35% of the Aghien lagoon catchment. High and very high LS values (5.69 - 225) are confined to only 3.05 % of the catchment area. These results correspond to the basin's

 ISSN: 1857-7881 (Print) e - ISSN 1857-7431

topography, which is predominantly flat, with low slopes observed across 85.95% of the area (slopes less than 10°) (**Table 10**). The high and very LS values are primarily located in the downstream part of the basin, where the relief is elevated, and near the main slopes of the Bété and Djibi rivers. The average LS value for the catchment is 1.84 (**Table 10; Figure 9**).

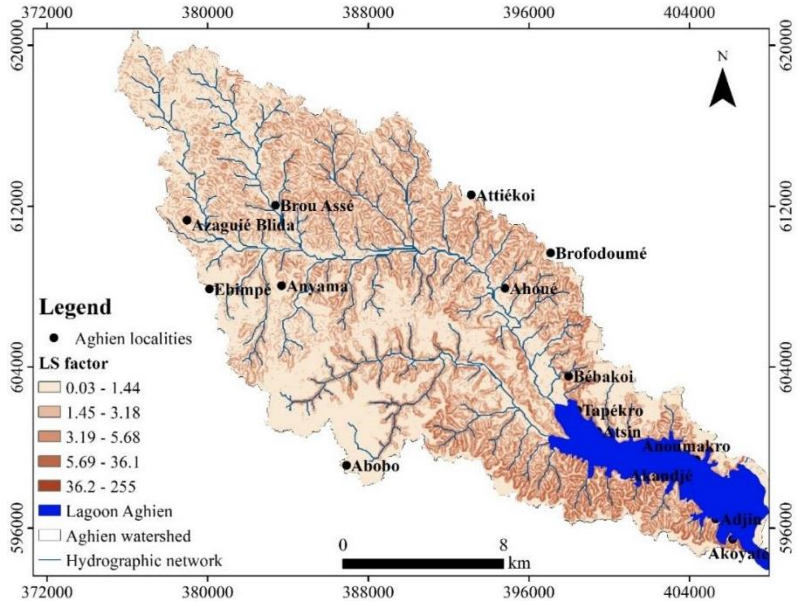

Figure 9. Spatial distribution of the LS Factor in Aghien lagoon watershed

Table 10. Topographic Factor

LS Factor	Area (ha)	Area (%)	Average
0.03-1.44	19891.7092	54.53	
1.45-3.18	9876.65	27.08	
3.19-5.68	5600.41079	15.35	1.84
5.69-36.10	1103.72266	3.03	
36.11-255	6.11952051	0.02	

Soil Erodibility K-factor

The calculated K-factor in the Aghien lagoon catchment area ranges from less than 0 to 0.26 t/ha/MJ/mm, with an average value of 0.13 t/ha/MJ/mm, which is relatively high (**Figure 10**; **Table 11**).

The lowest and low k-factor values are primarily found in the northern part and around the basin, covering 30.66% of the area. High to very high values are concentrated in regions with marl-clay soils, accounting for 24.53% of the basin area. The majority of the catchment area is characterized by modest K values, representing 44.81% of the total area.

 ISSN: 1857-7881 (Print) e - ISSN 1857-7431

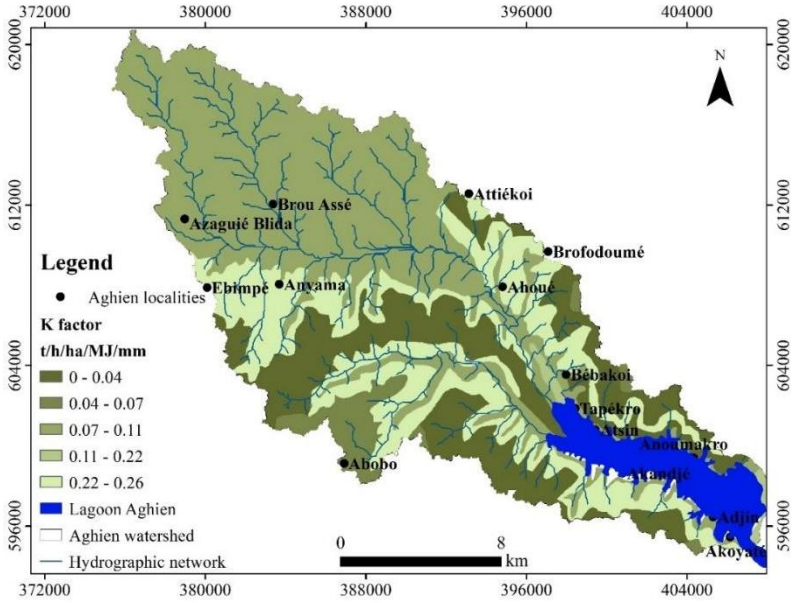

Figure 10. Spatial distribution of the K Factor in Aghien lagoon watershed

Table 11. Soil types and their K values in Aghien lagoon watershed

K factor (t/ha/MJ/mm)	Area (ha)	Area (%)	Average (t/ha/MJ/mm)	Soil type
0-0.04	9799.53	26.85		Ferrallitic sandy-clay soil
0.05-0.07	1391.58	3.81		Ferrallitic sandy soil
0.08-0.11	16356.36	44.81	0.13	Complex ferrallitic soil
0.18-0.22	350.88	0.96		hydromorph soil
0.23-0.26	8601.79	23.57		Ferrallitic sandy-clay soil

Crop Management Factor (C)

The values of the C-factor, scaled to the same level for comparison of the 2016 and 2020 maps, range from 0.02 and 1, with respective averages of 0.61 and 0.63, as shown in **Table 12** and **Figures 11**A and 11B. The maps indicate that the lowest C-factor values are associated with lower elevations. A significant portion of the catchment area exhibits high and very high C–factor values, ranging from 0.6 to 1, covering 54.16% and 51.95% of the area in 2016 and 2020, respectively. These areas are linked to bare soil, housing expansion, and market gardening activities. The spatial distribution of C-factor highlights the impact of anthropization due to human activities. Land use changes and rainfall variability have led to forest degradation, transforming these regions into cultivated land. The results reveal that 8.78% of the basin in 2016 and 6.73% in 2020 had very low vegetation cover, making these areas highly vulnerable to water erosion. Moderate C-factor values (0.4 - 0.6) account for 34.05% of the catchment area in 2016 and 41.31% in 2020, predominantly occupying the northern regions of the catchment.

 ISSN: 1857-7881 (Print) e - ISSN 1857-7431

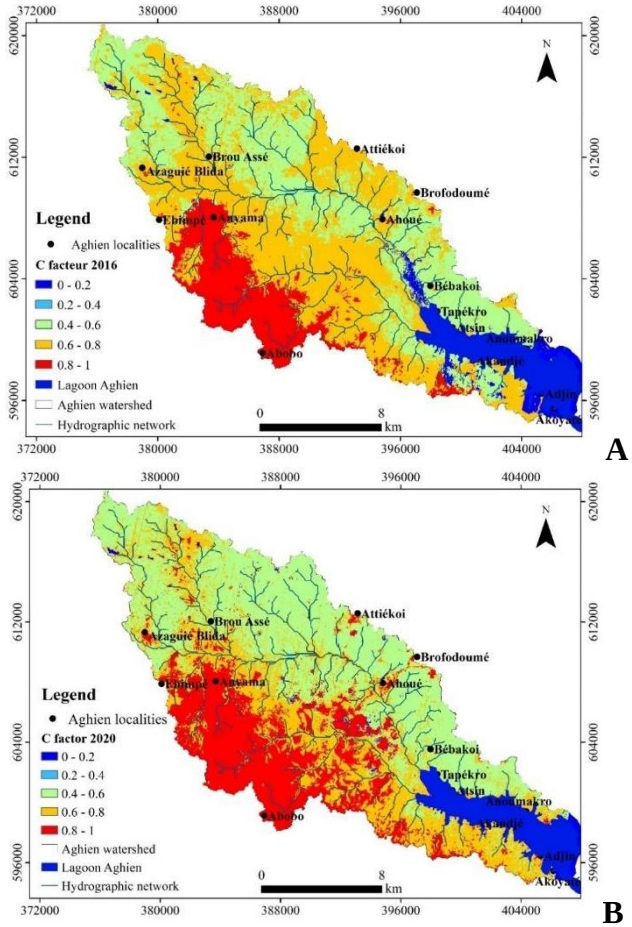

Figure 11. Spatial distribution of the C-factor in Aghien lagoon watershed (A: 2016; B: 2020)

Table 12. C-factor temporal evolution in Aghien lagoon watershed

	2016			2020		
C-factor	**Area (ha)**	**Area (%)**	**Average**	**Area (ha)**	**Area (%)**	**Average**
0 – 0.2	3206.61	8.78		2457.09	6.73	
0.2 – 0.4						
0.4 – 0.6	12431.87	34.05	0.61	15081.79	41.31	0.63
0.6 – 0.8	15980.22	43.77		11022.72	30.19	
0.8 – 1	4888.47	13.39		7945.42	21.76	

Conservation Practice (P) Factor

The value of the (dimensionless) P-factor ranges from 0 to 0.55, with an average of 0.29. This study revealed that 86.96% of the Aghien lagoon catchment area exhibited P-factor values between 0 and 0.3, representing very low to low values. Topographical features significantly influence erosion, as

 ISSN: 1857-7881 (Print) e - ISSN 1857-7431

lower P-factor values indicate more effective conservation practices in reducing soil erosion. High and very high P-factor values occupy only 1.58% of the catchment area, corresponding to the steepest slopes. The P-factor map, developed from the slope map, shows that the P-factor values are associated with topographical features. While the overall catchment area has relatively low P-factor values, higher values are concentrated around the Aghien lagoon (**Figure 12**; **Table 13**).

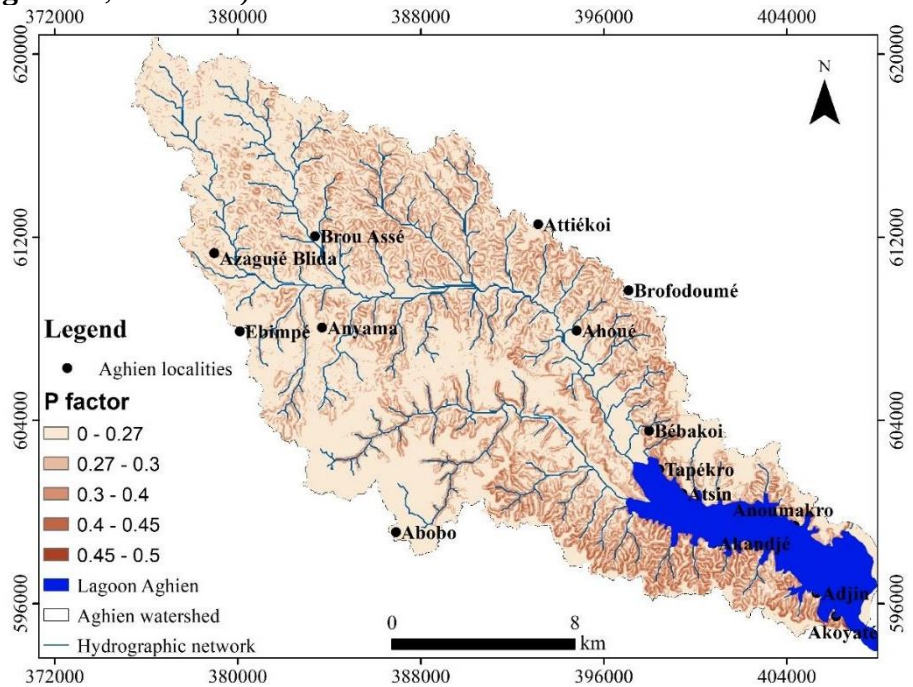

Figure 12. Spatial distribution of the P-Factor in Aghien lagoon watershed

Table 13. Conservation practice factor (P) values in Aghien lagoon watershed

P factor	Area (ha)	Area (%)	Average
0-0.27	24550.27	67.26	
0.28-0.3	7190.10	19.70	
0.31-0.4	4037.17	11.06	0.29
0.41-0.45	711.62	1.95	
0.46-0.5	10.83	0.03	

Soil Loss

The USLE layers derived for the R, K, LS, C, and P factors were integrated using the raster calculator tool in ArcGIS version 10.2 Spatial Analyst to quantify and generate soil erosion risk and severity maps for the Aghien lagoon watershed. The influence of environmental factors on the spatial distribution of soil erosion loss, including terrain units, elevation, slope, and land use/cover, was analyzed and evaluated.

 ISSN: 1857-7881 (Print) e - ISSN 1857-7431

The soil loss map produced was grouped into five categories: very low and low, moderate, and high to very high classes. The soil loss for the year 2016 was set to match the 2020 map for a better comparison. Soil loss varied between 0 and 9,230 t/ha/year, with an average of 60.65 t/ha/year in 2016 and 47.64 t/ha/year in 2020 (**Figures 13**A and 13B). The very low to low categories were dominant across almost the entire basin area, occupying 94.36% in 2016 and 95.77% in 2020 (**Table 14**). This class is distributed throughout the basin, in both low-lying and high-lying areas, with a slight increase of 1.47% observed from 2016 to 2020. On the other hand, the high and very high classes accounted for 0.95% and 0.65%, respectively in 2016 and 2020, showing a decrease of 46.15%. The moderate class occupied 4.69% of the 2016 basin area and 3.58% of the 2020 basin area. This class is located primarily on the slopes of watercourses and steep slopes along the Aghien lagoon.

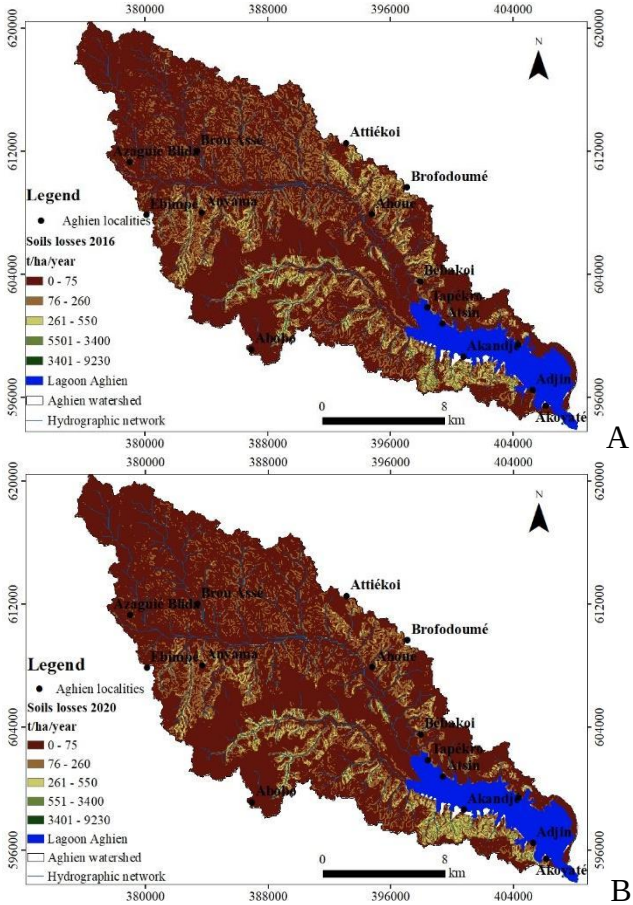

Figure 13. Spatial distribution of soil losses in Aghien lagoon watershed (A: 2016; B: 2020)

 ISSN: 1857-7881 (Print) e - ISSN 1857-7431

Table 14. Soil loss and erosion risk classes of the watershed

Soil loss (t/ha/year)	2016			2020			Erosion class
	Area (ha)	Area (%)	Average (t/ha/year)	Area (ha)	Area (%)	Average (t/ha/year)	
0-75	26095.03	71.49	60.65	28244	77.38	47.64	Very low
76-260	8346.49	22.87		6712.76	18.39		Low
261-550	1712.19	4.69		1305.77	3.58		Moderate
551-3400	345.69	0.95		237.36	0.65		High
3401-9230	0.61	0		0.10	0		Very high

Discussion

Soil loss maps derived from the USLE method (Wischmeier & Smith, 1978), based on the combination of the R, K, LS, C and P factors, were integrated using the raster calculator tool in the Spatial Analyst of ArcGIS version 10.2 to quantify and generate thematic soil erosion risk and severity maps for the Aghien lagoon watershed. The R-factor, representing the aggressiveness of precipitation, was higher in 2016 than in 2020. These high values can be attributed to the high annual precipitation recorded, ranging from 1,909 to 2,638 mm, as measured at various rainfall stations in the Aghien lagoon watershed. This rainfall follows a decreasing gradient from south to north towards the high altitudes (Khanchoula et al., 2020; Meliho et al., 2020). However, vegetation cover plays a crucial role in soil protection (Koua et al., 2019; Kilic, 2021), and soil without vegetation cover can be highly susceptible to rain (Coulibaly et al., 2021). The kinetic energy of raindrops is transformed on impact into mechanical energy capable of moving soil particles, even on very gentle slopes (Eblin et al., 2017). Under the effect of precipitation, particles break off and are carried downstream in areas of low depression, such as the Aghien lagoon (Dao et al., 2021). Increased rainfall and land use changes could increase the rate of soil erosion in the Aghien lagoon watershed (Maurya et al., 2021). In this area, soils are formed on soft materials such as marl and clay, which are not very permeable or impermeable, promoting runoff and soil erosion (Khemiri & Jebari, 2021). Additionally, the LS factor is essential for evaluating erosive potential (Meliho et al., 2020). Steeper slopes, often associated with lithology, increase soil losses with greater slope length and steepness (Almaaitah et al., 2018). In the study area, the steepest slopes are generally located on the banks of streams and adjacent valleys (Tsegaye & Bharti, 2021) within the Aghien lagoon watershed. However, the high and very high soil losses are relatively insignificant, accounting for 0.95% in 2016 and 0.65% in 2020. This drop in soil losses from 2016 to 2020 could be due to the increase in crop and fallow land from 33.92% in 2016 to 41.15% in 2020, marking a 17.56% increase. Most soil loss in the watershed

 ISSN: 1857-7881 (Print) e - ISSN 1857-7431

is attributed to moderate erosion, which accounts for 1,712.19 ha (4.69%) in 2016 and 1,305.77 ha (3.58%) in 2020 (Table 14), showing a decrease in the moderate class in 2020. On the other hand, the very low (71.49% in 2016 and 77.38% in 2020) and low (22.87% in 2016 and 18.29% in 2020) categories are scattered across the watershed. These low values are mainly observed on plateaus, plains, and low slopes, and are linked to the presence of significant vegetation cover, including crops and fallow land. This vegetation cover helps reduce the velocity of rain drops, promoting infiltration in the area (Dawa & Arjune, 2021) and significantly reducing the detachment of soil particles as well as runoff. A slight increase in the very low class was observed in 2020, which may be related to the increase in bare soil and habitats due to the expansion of the Autonomous District of Abidjan, despite lower rainfall in 2020 compared to 2016 (Figure 2). The vegetation cover in 2020 (41.15%) is higher than in 2016 (33.92%) (Table 8). According to Nut et al. (2021), bare soil can contribute to increased soil loss in a watershed. However, when examining the C-factor themes, a contrast is observed. This factor reveals that bare soil increased from 13.39% in 2016 to 21.76% in 2020, with an area of 2,981 ha (37.80%) 0f bare soil between 2016 and 2020. While bare soil can naturally favor soil loss, these areas are less contributory due to their location on plateaus or low-slope areas. The average soil loss values for the watershed over the study period are 60.65% in 2016 and 47.64% in 2020, with a regression in 2020. However, these average soil losses are higher than those found by Nut et al. (2021) in the Stung Sangkae watershed in Colombia (3.1 and 7.6 t/ha/year in 2002 and 2005, respectively); Sbai et al. (2021) in the Moulouya watershed in eastern Morocco (13.5 t/ha/year); and Tsegaye and Bharti (2021) in the Anjed watershed in northwest Ethiopia (17.3 t/ha/year).

Conclusion

The Universal Soil Loss Equation (USLE), combined with GIS techniques and remotely sensed data, has been successfully applied to determine soil erosion factors, including rainfall erosivity (R), soil erodibility (K), land cover (c), slope length and inclination (LS), and anti-erosion practices (P). The soil erosion map provides valuable information about sediment production through slope erosion and identifies areas susceptible to erosion. The potential erosion rate (t/ha/yr) obtained at the basin level was grouped into five classes: very low, low, moderate, high and very high risk. The assessment showed average losses of 60.65 t/ha/yr in 2016 and 47.64 t/ha/yr in 2020 for the Aghien lagoon basin. Soil loss varied from 0 to 9230 t/ha/year across the basin. Water erosion is visible in the Aghien lagoon basin, with more pronounced erosion on the slopes and reduced erosion in the plains, plateaus, and low or almost zero slopes. Low soil losses are linked to significant vegetation cover composed of crops and fallow land. The

 ISSN: 1857-7881 (Print) e - ISSN 1857-7431

comparison of specific degradation values reveals strong spatial disparity in the soil erosion rate, primarily due to lithology, vegetation cover, slope and catchment size. Most soil loss in the watershed is due to moderate erosion, occupying 1,712.19 ha (4.69%) in 2016 and 1,305.77 ha (3.58%) in 2020. The evolution of vegetation cover has had both negative and positive impacts on soil loss in the Aghien lagoon watershed. However, bare soil/habitats increased from 33.92% in 2016 to 41.15% in 2020.

Acknowledgements

We would like to express our gratitude to the "Debt Reduction and Development Contract" (C2D) between France and Côte d'Ivoire, which funded the research activities of the "Aghien Lagoon" project through the PReSeD-CI partnership. This partnership fostered excellent collaboration between researchers from the Université Nangui Abrogoua (UNA), particularly those from the "Laboratoire de Géosciences et Environnement" (LGE), and researchers from the French Institute for Research and Development (IRD).

Conflict of Interest: The authors reported no conflict of interest.

Data Availability: All data are included in the content of the paper.

Funding Statement: The authors did not obtain any funding for this research.

References:

1. Abé, J., N'doufou, G. H. C., Konan, K. E., Yao, K. S., & Bamba, S. B. (2014). Relations entre les points critiques d'érosion et le transit littoral en Côte d'Ivoire. Africa Geoscience Review. 21(1-2). 1-14.
2. Adopo, K. L., Akobe, A. C., Etche, M., Monde, S., & Aka, K. (2014). Situation de l'érosion Côtière au Sud-est de la Côte d'Ivoire. entre Abidjan et Assinie. Revue Ivoirienne de Science et Technologie. 24. 223-237.
3. Aké, G. É., Kouadio, B. H., Adja, M. G., Ettien, J. B., Effebi K. R., & Biémi, J. (2012). Cartographie de la vulnérabilité multifactorielle à l'érosion hydrique des sols de la région de Bonoua (Sud-Est de la Côte d'Ivoire). *Physio-Géo. Géographie physique et environnement.* (Volume 6). 1-42. https://doi.org/10.4000/physio-geo.2285
4. Almaaitah, R., Azhari, A., & Asri, R. (2018). Spatial Distribution Of Soil Erosion Risk Using Rusle, Rs And Gis Techniques. *International Journal of Civil Engineering and Technology*, 9(10), 681-697. http://www.iaeme.com/IJCIET/index.as

 ISSN: 1857-7881 (Print) e - ISSN 1857-7431

5. Anache, J. A. A., Bacchi, C. G. V., Panachuki, E., & Sobrinho T. A. (2016). Assessment of methods for predicting soil erodibility in soil loss modeling. Geociências (São Paulo), 34(1), 32-40.
6. Batista, P. V. G., Silva, M. L. N., Silva, B. P. C., Curi, N., Bueno, I. T., Júnior, F. W. A., & Quinton, J. (2017). Modelling spatially distributed soil losses and sediment yield in the upper Grande River Basin-Brazil. *Catena*, 157, 139-150. http://dx.doi.org/10.1016/j.catena.2017.05.025
7. Belaout, F., Mekerta, B., Zentar, R., Chabani, A., Abdelkrimi, A., & Kalloum, S. (2021). Modeling of erosion in the Wadi Guir watershed (South-West Algeria) by the application of Geographic Information System (GIS). International Journal of Forest. Soil and Erosion. 11(1).
8. Benchettouh, A., Kouri, L., & Jebari, S. (2017). Spatial estimation of soil erosion risk using RUSLE/GIS techniques and practices conservation suggested for reducing soil erosion in Wadi Mina watershed (northwest. Algeria). *Arabian Journal of Geosciences*. 10(4). 79. http://dx.doi.org/10.5772/intechopen.96190
9. Biswas, S. S. & Pani, P. (2015). Estimation of soil erosion using RUSLE and GIS techniques: a case study of Barakar River basin, Jharkhand, India. Modeling Earth Systems and Environment, 1(4), 1-13. DOI 10.1007/s40808-015-0040-3
10. Bollinne, A. & Laurant, A. (1983). La prévision de l'érosion en Europe Atlantique : le cas de la zone limoneuse de Belgique. Pédologie, XXXIII, 2, 117-136pp.
11. Bollinne, A. & Rosseau, P. (1978). Erodibilité des sols de moyenne et haute Belgique. Utilisation d'une méthode de calcul du facteur K de l'équation universelle de perte en terre. Bull. Soc. Géogr. de Liège, 14,4 : 127-140pp.
12. Bouguerra, H., Bouanani, A., Khanchoul, K., Derdous, O., & Tachi, S. E. (2017). Mapping erosion prone areas in the Bouhamdane watershed (Algeria) using the Revised Universal Soil Loss Equation through GIS. Journal of water and land development. 32(1). 13-23pp.
13. Boukheir, R., Cerdo, O., & Abdallah, C. (2006). Regional soil erosion risk mapping in Lebanon. The Journal of Geomorphology. Vol. 82. Iss. 3 p. 347–359.
14. Coulibaly, L. K., Guan, Q., Assoma, T. V., Fan, X., & Coulibaly, N. (2021). Coupling linear spectral unmixing and RUSLE2 to model soil erosion in the Boubo coastal watershed, Côte d'Ivoire. *Ecological Indicators*, 130, 108092. https://doi.org/10.1016/j.ecolind.2021.108092
15. Dao, A., Koffi, E. S., Noufé, D. D., Kamagaté, B., Goné, L. D., Séguis, L., & Perrin, J. L. (2021). Soil loss vulnerability: the case study of

 ISSN: 1857-7881 (Print) e - ISSN 1857-7431

Aghien lagoon watershed outskirts Abidjan city (Côte d'Ivoire). *Proceedings of the International Association of Hydrological Sciences*, 384, 121-126. https://doi.org/10.5194/piahs-384-121-2021

16. Das, B., Bordoloi, R., Thungon, L. T., Paul, A., Pandey, K. P., Mishra, M., & Tripathi O. P. (2020). An integrated approach of GIS. RUSLE and AHP to model soil erosion in West Kameng watershed. Arunachal Pradesh. J. *Earth Syst. Sci.* (2020) 129:94. https://doi.org/10.1007/s12040-020-1356-6
17. Dawa, D. & Arjune, V. (2021). Identifying Potential Erosion-Prone Areas in the Indian Himalayan Region Using the Revised Universal Soil Loss Equation (RUSLE). *Asian Journal of Water, Environment and Pollution*, 18(1), 15-23. DOI : 10.3233/AJW210003
18. Déguy, J. P. A., N'Go, A. Y., Kouassi, H. K., Soro, E. G., & Goula, A. T. B. (2018). Contribution of a Geographical Information System to the Study of Soil Loss Dynamics in the Lobo Catchment (Côte d'Ivoire). *Journal of Geoscience and Environment Protection*. 6(09). 183. doi: 10.4236/gep.2018.69014.
19. Desmet, P. J. J. & Govers, G. (1996). A GIS procedure for automatically calculating the USLE LS factor on topographically complex landscape units. *Journal of soil and water conservation*, *51*(5), 427-433.
20. Eblin, S. G., Yao, A. B., Anoh, K. A., & Soro, N. (2017). Cartographie de la vulnérabilité multifactorielle aux risques d'érosion hydrique des sols de la région d'Adiaké. sud-est Côtier de la côte d'ivoire. *Revue Internationale des Sciences et Technologie.* 30. 197-216.
21. EL Garouani, A., Chen, H., Lewis, L., Tribak, A., & Abharour, M. (2008). Cartographie de l'utilisation du sol et de l'érosion nette à partir d'images satellitaires et du SIG IDRISI au nord-est du Maroc. Télédétection. Editions scientifiques GB. 8 (3), 193-201 pp.
22. Ganasri, B. P. & Ramesh, H. (2016). Assessment of Soil Erosion by RUSLE Model Using Rmote Sensing and GIS – A Case Study of Nethravathi. *Basin Geoscience Frontiers*, 7:953-961. https://doi.org/10.1016/j.gsf.2015.10.007
23. Kayet, N., Pathak, K., Chakrabarty, A., & Sahoo, S. (2018). Evaluation of soil loss estimation using the RUSLE model and SCS-CN method in hillslope mining areas. International Soil and Water Conservation Research, 6(1), 31-42. https://doi.org/10.1016/j.iswcr.2017.11.002
24. Karydas, C. G., Sekuloska, T., & Silleos, G. N. (2009). Quantification and site-specification of the support practice factor when mapping soil erosion risk associated with olive plantations in the Mediterranean island of Crete. *Environmental Monitoring and Assessment*, 149, 19-28. https://doi.org/10.1007/s10661-008-0179-8

 ISSN: 1857-7881 (Print) e - ISSN 1857-7431

25. Khanchoula, K., Selmi, K., & Benmarce, K. (2020). Assessment of soil erosion by RUSLE model in the Mellegue watershed, northeast of Algeria. *Environment and Ecosystem Science* (EES), 4(1), 15-22. http://doi.org/10.26480/ees.01.2020.15.22
26. Khemiri, K. & Jebari, S. (2021). Évaluation de l'érosion hydrique dans des bassins versants de la zone semi-aride tunisienne avec les modèles RUSLE et MUSLE couplés à un Système d'information géographique. *Cah. Agric*. 30: 7. https://doi.org/10.1051/cagri/2020048
27. Kilic, O. M. (2021). Effects of land use and land cover changes on soil erosion in semi-arid regions of Turkey; a case study in Almus Lake watershed. *Carpathian Journal of Earth and Environmental Sciences*, 16(1), 129-138. DOI: 10.26471/cjees/2021/016/161
28. Kinnell, P. I. A. (2016). A review of the design and operation of runoff and soil loss plots. Catena 145 (2016) 257-265. 10.1016/j.catena.2016.06.013. http://dx.doi.org/10.1016/j.catena.2016.06.013
29. Koffi, E. S., Koffi, K. J. T., Perrin, J-L., Séguis, L., Guilliod, M., Goné, D. L., & Kamagaté, B. (2019). Hydrological and water quality assessment of the Aghien Lagoon hydrosystem (Abidjan. Côte d'Ivoire). *Hydrological Sciences Journal*, 64:15. 1893-1908. https://doi.org/10.1080/02626667.2019.1672875
30. Koffi, K. J. P., N'Go, Y. A., Yéo K. M., Koné, D., & Savané, I. (2014). Détermination des périmètres de protection de la lagune Aghien par le calcul du temps de transfert de l'eau jusqu' à la lagune. *Larhyss Journal* 2 19. 19–3.
31. Koua, J. J. T., Anoh, A. K., Soro, D. T., Kouamé, J. K., & Jourda, R. J. P. (2019). Evaluation of Agricultural Practices Scenarios for Reducing Erosion in Buyo Lake Catchment (Sassandra; Côte d'Ivoire) by Use of GIS. *Journal of Geoscience and Environment Protection*. 7(7). 154-171. https://doi.org/10.4236/gep.2019.77011
32. Kouadio, B. H., Kouamé, K. F., Saley, B. M., & Biémi, J. (2007). Traoré Ibrahima1Insécurité climatique et géorisques en Côte d'Ivoire : étude du risque d'érosion hydrique des sols dans la région semi-montagneuse de Man (Ouest de la Côte d'Ivoire). Sécheresse vol. 18. n° 1 : 29-37.
33. Kouadio, Z. A. (2018). Spatial Analysis of Erosive Runoff in the Mé Watershed (Côte d'Ivoire). Journal of Water Science and Environment Technologies. 3(02). 376-382.
34. Kouassi, K. H., Koua, T. J. J., Zro, B. G. F., & N'Go, Y. A. (2020). Contribution of a Geographical Information System to the study of soil erosion by water in the watershed of the hydro-agricultural dam of

 ISSN: 1857-7881 (Print) e - ISSN 1857-7431

Babadou (Côte d'Ivoire). International Journal of Innovation and Applied Studies. 28(2). 458-467.

35. Koukougnon, W. G., Brou, K. M., Silué, Y., & Della André, A. L. L. A. (2021). Korhogo à l'épreuve de l'érosion et ses conséquences (nord-Côte d'Ivoire). International Journal of Humanities and Cultural Studies (IJHCS) ISSN 2356-5926. 8(2). 37-50.
36. Markhi, A., Laftouhi, N-E., Soulaimani, A., & Fniguire, F. (2015). Quantification et évaluation de l'érosion hydrique en utilisant le modèle RUSLE et déposition intégrée dans un SIG. Application dans le bassin versant n'fis dans le haut atlas de Marrakech (Maroc). European Scientific Journal, edition vol.11. No.29 ISSN: 1857-7881pp.
37. Maurya, S., Srivastava, P. K., Yaduvanshi, A., Anand, A., Petropoulos, G. P., Zhuo, L., & Mall, R. K. (2021). Soil erosion in future scenario using CMIP5 models and earth observation datasets. *Journal of Hydrology*, 594, 125851. https://doi.org/10.1016/j.jhydrol.2020.125851
38. Mazouzi, K., El-Hmaidi, A., Bouabid, R., & El-Faleh, E-M. (2021). Quantification de l'érosion hydrique par la méthode RUSLE au niveau du bassin versant de l'Oued Mikkès en amont du barrage Sidi Chahed (région de Meknès. Maroc). *European Scientific Journal,* ESJ. 17(14). 256. https://doi.org/10.19044/esj.2021.v17n14p256
39. Meliho, M., Khattabi, A., & Mhammdi, N. (2020). Spatial assessment of soil erosion risk by integrating remote sensing and GIS techniques: a case of Tensift watershed in Morocco. *Environmental Earth Sciences*, 79(10), 1-19. https://doi.org/10.1007/s12665-020-08955-y
40. Meliho, M., Khattabi, A., Mhammdi, N., & Zhang, H. (2016). Cartographie des risques de l'erosion hydrique par l'Equation Universelle Revisee des Pertes en Sols, la teledetection et les SIG dans le bassin versant de l'ourika (Haut Atlas, Maroc), *Eur. Scient. J*., 12, 32, https://doi.org/10.19044/esj.2016.v12n32p277
41. N'Dri, W. K. C., Pistre, S., Jourda, J. P., & Kouamé, K. J. (2021). Application of a Deterministic Distributed Hydrological Model for Estimating Impact of Climate Change on Water Resources in Côte d'Ivoire Using RCP 4.5 and RCP 8.5 Scenarios: Case of the Aghien Lagoon. Dr. Mustafa Turkmen; Dr. Kwong Fai Andrew Lo. International Research in Environment, Geography and Earth Science Vol. 9, 9, Book Publisher International (a part of SCIENCEDOMAIN International), pp.129 - 153, 2021, 978-93-91215-91-0. ff10.9734/bpi/ireges/v9/5512dff. ffhal-03254861f
42. Nana, P. P. (2018). Du groupe à l'individu : dynamique de la gestion foncière en pays gouin (sud-ouest du Burkina Faso), Belgeo URL

 ISSN: 1857-7881 (Print) e - ISSN 1857-7431

http://journals,openedition,org/belgeo/21653 6080; https://doi.org/10.4000/belgeo.26080

43. N'Dri, B. É., Niamké, K. H., Koudou, A., & N'Go, Y. A. (2017). Cartographie des formes d'érosion hydrique dans la commune urbaine d'attécoubé (Abidjan. Côte d'Ivoire) /mapping of water erosion forms in the urban district of Attecoube (Abidjan. Côte d'Ivoire). International Journal of Innovation and Applied Studies. 19(4). 960.
44. Nut, N., Mihara, M., Jeong, J., Ngo, B., Sigua, G., Prasad, P. V., & Reyes, M. R. (2021). Land use and land cover changes and its impact on soil erosion in Stung Sangkae catchment of Cambodia. *Sustainability*, 13(16), 9276. https://doi.org/10.3390/su13169276
45. Onyando, J O., Kisoyan, P., & Chemelil, M. C. (2005). Estimation of potential soil erosion for river Perkerra catchment in Kenya; *Water Resour. Manag*. 19(2) 133–143. https://doi.org/10.1007/s11269-005-2706-5
46. Panagos, P., Borrelli, P., Meusburger, K., Alewell, C., Lugato, E., & Montanarella, L. (2015a). Estimating the soil erosion cover-management factor at the European scale. Land use policy, 48, 38-50. http://dx.doi.org/10.1016/j.landusepol.2015.05.021
47. Panagos, P., Borrelli, P., Poesen, J., Ballabio, C., Lugato, E., Meusburger, K., & Alewell, C. (2015b). The new assessment of soil loss by water erosion in Europe. Environmental science and policy, 54, 438-447. https://doi.org/10.1016/j.envsci.2015.08.012
48. Payet, E., Dumas, P., & Pennober, G. (2012). Modélisation de l'érosion hydrique des sols sur un bassin versant du sud-ouest de Madagascar, le Fiherenana. VertigO: la revue électronique en sciences de l'environnement, 11(3). https://id.erudit.org/iderudit/1015047ar
49. Piyathilake, I. D. U. H., Sumudumali, R. G. I., Udayakumara, E. P. N., Ranaweera, L. V., Jayawardana, J. M. C. K., & Gunatilake, S. K. (2021). Modeling predictive assessment of soil erosion related hazards at the Uva province in Sri Lanka. Modeling Earth Systems and Environment, 7(3), 1947-1962. . https://doi.org/10.1007/s40808-020-00944-1
50. Renard, K. G. & Freimund, J. R. (1994). Using monthly precipitation data to estimate the R-factor in the revised USLE. Journal of hydrology, 157(1-4), 287-306.
51. Renard, K. G., Foster, G. R., Weesies, G. A., McCool, D. K., & Yoder, D. C. (1996). Predicting soil erosion by water: A guide to conservation planning with the Revised Universal Soil Loss Equation (RUSLE). Agriculture handbook, 703, 25-28.
52. Roose, E. J. & Lelong, F. (1976). Les facteurs de l'érosion hydrique en Afrique Tropicale. Études sur petites parcelles expérimentales de sol.

 ISSN: 1857-7881 (Print) e - ISSN 1857-7431

Revue de géographie physique et de géologie dynamique. Vol. 18. Iss. 4 p. 365–374.

53. Roose, E. J. (1977). Use of the Universal Soil Loss Equation to Predict Erosion in West Africa. In Soil erosion: Prediction and control. Soil Conservation Society of America, Special Publication no. 21. Ankeny, Iowa.
54. Rougerie, G. (1958). Modalité du ruissellement sous forêt dense de Côte d'Ivoire. CR Acad Sci Paris ; 246 : 290-2.
55. Rougerie, G. (1960). Le façonnement actuel des modelés en Côte d'Ivoire forestière. Mémoire IFAN 58. Dakar : Institut Fondamental d'Afrique Noire (IFAN).
56. Sbai, A., Mouadili, O., Hlal, M., Benrbia, K., Zahra Mazari, F., Bouabdallah, M., & Saidi, A. (2021). Water Erosion in the Moulouya Watershed and its Impact on Dams' Siltation (Eastern Morocco). Proceedings of the International Association of Hydrological Sciences, 384, 127-131.
57. Songu, G. A., Abu, R. D., Temwa, N. M., Yiye S. T., Wahab, S., & Mohammed, B. G. (2021). Analysis of Soil Erodibility Factor for Hydrologic Processes in Kereke Watershed, North Central Nigeria. *Journal of Applied Sciences and Environmental Management*, 25(3), 425-432. https://dx.doi.org/10.4314/jasem.v25i3.18
58. Stone, R. P. & Hilborn, D. (2000). Universal Soil Loss Equation-Factsheet. http://www.omafra.gov.on.ca/english/engineer/facts/00-001.htm
59. Swarnkar, S., Malini, A., Tripathi, S., & Sinha, R. (2018). Assessment of uncertainties in soil erosion and sediment yield estimates at ungauged basins: an application to the Garra River basin, India. *Hydrology and Earth System Sciences*, 22(4), 2471-2485. https://doi.org/10.5194/hess-22-2471-2018
60. Tian, Y. C., Zhou, Y. M., Wu, B. F., & Zhou, W. F. (2009). Risk assessment of water soil erosion in upper basin of Miyun Reservoir, Beijing, China. *Environmental Geology*, *57*, 937-942. https://doi.org/10.1007/s00254-008-1376-z
61. Toumi, S., Meddi, M., Mahé, G., & Brou, Y-T. (2013). Cartographie de l'érosion dans le bassin versant de l'Oued Mina en Algérie par télédétection et SIG. *Hydrological Sciences Journal,* l58. 01- 17. https://doi.org/10.1080/02626667.2013.824088.
62. Traoré, A., Soro, G., Kouadio, E. K., Bamba, B. S., Oga, M. S., Soro, N., & Biémi, J. (2012). Evaluation des paramètres physiques. chimiques et bactériologiques des eaux d'une lagune tropicale en période d'étiage : la lagune Aghien (Côte d'Ivoire). *International*

 ISSN: 1857-7881 (Print) e - ISSN 1857-7431

Journal of Biological and Chemical Sciences. 6(6). 7048-7058. http://dx.doi.org/10.4314/ijbcs.v6i6.40

63. Trimble (2010). eCognition® Developer 8.64.0 Reference Book. (Available at: http://www.definiens.com/ . Access on may 11, 2015)
64. Tsegaye, L. & Bharti, R. (2021). Soil erosion and sediment yield assessment using RUSLE and GIS-based approach in Anjeb watershed, Northwest Ethiopia. *SN Applied Sciences*, 3(5), 1-19. https://doi.org/10.1007/s42452-021-04564-x
65. Vrieling, A. (2005). Satellite remote sensing for water erosion assessment. a review. CATENA. Vol. 65. Iss. 1 p. 2–18
66. Wachal, D. J., Banks, K. E., Hudak, P. F., & Harmel, R. D. (2009). Modeling erosion and sediment control practices with RUSLE 2.0 : A management approach for natural gas well sites in Denton County. TX. USA. *Environmental geology*. 56(8). 1615-1627pp. https://doi.org/10.1007/s00254-008-1259-3
67. Wischmeier, V. H. & Smith, D. D. (1978). Predicting rainfall erosion losses- a guide to conservation planning. United States Department of Agriculture in cooperation with Purdue Agricultural Experiment Station. United States Department of Agriculture. Washington. Agriculture Handbook No. 282.
68. Zhou, P., Luukkanen, O., Tokola, T., & Nieminen, J. (2008). EAect of vegetation cover on soil erosion in a mountainous watershed; *Catena* 75(3) 319–325pp. https://doi.org/10.1016/j.catena.2008.07.010